



HAL
open science

Synthesis and characterization of analogues of glycine-betaine ionic liquids and their use in the formation of aqueous biphasic systems

Matheus Pereira, Sónia Pedro, Joana Gomes, Tania E. Sintra, Sónia P.M. Ventura, João A.P. Coutinho, Mara G. Freire, Aminou Mohamadou

► To cite this version:

Matheus Pereira, Sónia Pedro, Joana Gomes, Tania E. Sintra, Sónia P.M. Ventura, et al.. Synthesis and characterization of analogues of glycine-betaine ionic liquids and their use in the formation of aqueous biphasic systems. *Fluid Phase Equilibria*, 2019, 494, pp.239-245. 10.1016/j.fluid.2019.05.001 . hal-02429718

HAL Id: hal-02429718

<https://hal.univ-reims.fr/hal-02429718v1>

Submitted on 25 Oct 2021

HAL is a multi-disciplinary open access archive for the deposit and dissemination of scientific research documents, whether they are published or not. The documents may come from teaching and research institutions in France or abroad, or from public or private research centers.

L'archive ouverte pluridisciplinaire **HAL**, est destinée au dépôt et à la diffusion de documents scientifiques de niveau recherche, publiés ou non, émanant des établissements d'enseignement et de recherche français ou étrangers, des laboratoires publics ou privés.



Distributed under a Creative Commons Attribution - NonCommercial 4.0 International License

1 **Synthesis and characterization of analogues of glycine-betaine ionic liquids and**
2 **their use in the formation of aqueous biphasic systems**

3
4 **Matheus M. Pereira¹, Sónia N. Pedro¹, Joana Gomes¹, Tânia E. Sintra¹, Sónia P. M. Ventura¹,**
5 **João A. P. Coutinho¹, Mara G. Freire¹, Aminou Mohamadou^{2*}**

6

7

8 ¹CICECO – Aveiro Institute of Materials, Department of Chemistry, University of Aveiro, Campus
9 Universitário de Santiago, 3810-193 Aveiro, Portugal

10 ²Institut de Chimie Moléculaire de Reims (ICMR), UMR CNRS 7312, Université de Reims
11 Champagne-Ardenne, Moulin de la Housse, BP 1039 – 51687 Reims cedex 2, France.

12

13

14

15

16 * Corresponding author: Tel: +33 (0)32691 3334; Fax: +33 (0)32691 3243

17

E-Mail : aminou.mohamadou@univ-reims.fr (A. Mohamadou)

18

19

20

21

22 **Abstract**

23 A series of novel analogues of glycine-betaine ionic liquids (AGB-ILs), viz. 1-(4-ethoxy-4-oxobutyl)-1-
24 methylpyrrolidin-1-ium, N,N,N-tri(*n*-butyl)(4-ethoxy-4-oxobutyl)-1-phosphonium and N,N,N-
25 trialkyl(4-ethoxy-4-oxobutyl)-1-aminium cations with ethyl, *n*-propyl and *n*-butyl alkyl chains,
26 combined with the bromide anion, have been synthesized and characterized. Their synthesis and
27 characterization by spectroscopic methods and elemental analysis is here reported. These ILs were
28 further characterized in what concerns their thermal properties and ecotoxicity against *Allvibrio fischeri*,
29 and compared with the commercial tetra(*n*-butyl)ammonium and tetra(*n*-butyl)phosphonium bromide.
30 The novel AGB-ILs described in this work have low melting points, below 100 °C, display high
31 degradation temperatures (180-310 °C), and low toxicity as shown by being harmless or practically
32 harmless towards the marine bacteria *Allvibrio fischeri*. Finally, the ability of the synthesized AGB-ILs
33 to form aqueous biphasic systems with potassium citrate/citric acid (at pH 7) was evaluated, and the
34 respective ternary phase diagrams were determined. It is shown that the increase of the cation alkyl
35 chain length facilitates the creation of ABS, and that phosphonium-based ILs present a slightly better
36 separation performance in presence of aqueous solutions of the citrate-based salt.

37

38

39 *Key words:* Ionic liquids, analogues of glycine-betaine, thermal properties, ecotoxicity, *Allvibrio*
40 *fischeri*, aqueous biphasic systems, phase diagram.

41

42

43

44

45

46

47 **1. Introduction**

48 In order to replace volatile organic solvents, which may be harmful to both the process operators and
49 the environment [1], many researchers have focused on the development of “greener solvents” [2].
50 Amongst these solvents, aprotic ionic liquids (ILs) are an interesting class of fluids since, if properly
51 designed, they display a negligible vapour pressure at ambient conditions, non-flammability, high
52 chemical and thermal stabilities, and unique solvation capabilities. As a result of these features, they
53 have attracted attention as solvents for chemical and electrochemical reactions, biphasic catalysis,
54 chemical syntheses, separation processes, among others [3-6]. Nevertheless, some ILs may display
55 some toxicity and cause biodegradability concerns [7, 8]. Therefore, the design of more
56 environmentally benign ILs has been a hot topic over the past years [9]. To obtain “greener” ILs, the
57 starting materials should be non-toxic and renewable, and their synthesis environmentally-friendly [10].
58 The synthesis of ILs from renewable raw materials is more beneficial and attractive compared to the use
59 of compounds derived from fossil feedstocks. In recent years, several bio-based ILs with biocompatible
60 character have been synthesized and characterized, receiving considerable attention for distinct
61 applications [11, 12]. Cholinium based-ILs emerged in several reports as biocompatible alternatives
62 over the well-known imidazolium-based counterparts on the dissolution of biomass, CO₂ absorption
63 processes or biomaterials development [13-15]. More recently, amino-acid- and carbohydrate-based ILs
64 have been proposed to improve the biocompatible properties of ILs. The first have been tested in the
65 pretreatment of lignocellulosic materials and as catalysts in organic synthesis [16-19], while the later
66 have recently been proposed as novel chiral solvents [20, 21].

67 Previously, we reported the synthesis and characterization of ILs wherein the cation is either an
68 alkyl ester glycine-betaine (GB) [22] or an analogue of glycine-betaine (AGB) [23], in which the
69 ammonium cation comprises three alkyl groups and an ethyl acetate group. Hydrophobic GB-ILs have
70 been applied in liquid-liquid extraction of pesticides [24], while AGB-ILs were employed in the
71 extraction of metals from aqueous solutions [25-27]. On the other hand, hydrophilic (water-miscible)
72 AGB-ILs have been used in the extraction of value-added compounds from biomass [28]. The
73 cytotoxicity of these ILs aqueous solutions containing the biomass extracts was assessed in a
74 macrophage cell line, as well as their anti-inflammatory potential via reduction of lipopolysaccharide-
75 induced cellular oxidative stress, showing that the IL aqueous solutions enriched in the biomass extracts
76 display higher antioxidant and anti-inflammatory effects than the recovered solid extracts, and that these
77 solutions may be used in nutraceutical and cosmetic applications [28].

78 Glycine-betaine, which is a zwitterionic acetate group bearing a quaternary
79 tri(methyl)ammonium, can be found in sugar beet molasses (up to 27 wt%) after the extraction of
80 saccharose [29]. These organic osmolytes are recognized by their accumulation in a wide variety of
81 plants in response against environmental stress. They have positive effects on enzyme and membrane

82 integrity along with adaptive roles in mediating osmotic adjustment in plants growing under stress
 83 conditions [30, 31]. Furthermore, glycine-betaine and their derivatives are currently used as food
 84 supplements [32], as well as in cosmetic lotions and formulations [33]. Given the benefits and “green”
 85 credentials associated to glycine-betaine, we hereby report on the synthesis and characterization of 5
 86 new bromide-based AGB-ILs, in which the cation carries an ethyl ester butyrate and three alkyl groups.
 87 Two commercial ILs, namely tetrabutylammonium bromide and tetrabutylphosphonium bromide, were
 88 also investigated for comparison purposes. The AGB-ILs synthesis and characterization are reported,
 89 and their thermal properties, such as melting point, glass transition temperature and decomposition
 90 temperature, were determined. The ecotoxicity of the synthesized AGB-ILs towards *Allvibrio fischeri*
 91 was assessed using the Microtox[®] acute toxicity test [34, 35]. Finally, while envisaging their application
 92 in separation processes, their ability to create aqueous biphasic systems (ABS) in presence of potassium
 93 citrate was investigated.

94

95 **2. Experimental Section**

96 **2.1. Materials**

97 All used chemicals are described in Table 1, which comprises the CAS number, molecular
 98 weight, purity and supplier.

99 **Table 1**

100 Name, CAS number, molecular weight, purity and supplier of the used chemicals.

Reagents	CAS number	Molecular weight	Purity (%)	Supplier
N-methylpyrrolidine	121-44-8	85.15	≥ 97	Sigma Aldrich
triethylamine	121-44-8	101.19	> 99	Fischer Scientific
tri(<i>n</i> -propyl)amine	102-69-2	143.27	≥ 98	Sigma Aldrich
tri(<i>n</i> -butyl)amine	102-82-9	185.35	≥ 98	Fischer Scientific
4-bromobutyric acid ethyl ester	2969-81-5	195.05	≥ 97	Sigma Aldrich
tripotassium citrate monohydrate	6100-05-6	324.42	≥ 99	Fischer Scientific
citric acid monohydrate·H ₂ O	5949-29-1	210.14	100	Sigma Aldrich
tetrabutylammonium bromide	1643-19-2	322.37	> 97	Fluka
tetrabutylphosphonium bromide	3115-68-2	339.33	> 98	Sigma Aldrich

101

102

103 2.2. Synthesis of AGB-ILs

104 2.2.1. 1-(4-ethoxy-4-oxobutyl)-1-methylpyrrolidin-1-ium bromide ([MepyrNC₄]Br · H₂O)

105 A solution of 4-bromobutyrate acid ethyl ester (42.9 g, 0.22 mol) in ethyl acetate (100 mL) was added
106 to a solution of N-methylpyrrolidine (29.8 g, 0.35 mol) in 110 mL of ethyl acetate. The mixture was
107 stirred at room temperature for 24 days. The precipitate produced during the reaction was filtered, and
108 washed twice with ethyl acetate and then with ethyl ether, and dried under vacuum. Yield (54.5 g,
109 83%). Elemental analysis: Found: C, 44.40; H, 7.80; N, 4.70%. Calculated for C₁₁H₂₄BrNO₃ (MW =
110 298.22 g·mol⁻¹): C, 44.30; H, 8.11; N, 4.70%. ¹H NMR, δ/ppm (300 MHz, DMSO-*d*₆): 1.20 [3 H, t,
111 CH₃(β)]; 2.01 [2 H, m, CH₂(2)]; 2.08 (2 H, s, CH₃(c)]; 2.41 [2 H, t, CH₂(3)]; 3.38 [2 H, m, CH₂(b)];
112 3.56 (6 H, m, CH₂(a+1)]; 4.09 (2 H, q, CH₂(α)). ¹³C NMR, δ/ppm (75.47 MHz, DMSO-*d*₆): 11.2
113 [CH₃(β)]; 14.8 [CH₃(c)]; 19.1 [CH₂(2)]; 21.7 [CH₂(3)]; 23.0 [CH₂(1)]; 31.3 [CH₂(b)]; 56.9 3 [CH₂(a)];
114 60.5 [CH₂(α)]; 172.5 [C=O(4)]. ESI-MS, m/z Found (Calculated): 200.16 (200.30) [C₁₁H₂₂NO₂⁺];
115 115.07 (115.15) [C₆H₁₁O₂⁺]. IR (v/cm⁻¹): 3390 (ν_{O-H}); 2955, 2870 (ν_{C-H}); 1720 (ν_{C=O}); 1286 (ν_{C-N}).

116

117 2.2.2. N,N,N-tri(*n*-alkyl)(4-ethoxy-4-oxobutyl)-1-aminium bromide

118 Tri(ethyl)[4-ethoxy-4-oxobutyl]ammonium bromide and Tri(*n*-propyl)[4-ethoxy-4-oxobutyl]ammonium
119 bromide were synthesized as described for (N-methylpyrrolidyl-4-ethoxy-4-oxobutyl)ammonium
120 bromide using tri(ethyl)amine (35.4 g, 0.35 mol) and tri(*n*-propyl)amine (50.1 g, 0.35 mol),
121 respectively.

122

123 2.2.2.1. N,N,N-tri(ethyl)(4-ethoxy-4-oxobutyl)-1-aminium bromide ([Et₃NC₄]Br · 0.2 H₂O)

124 Yield (52.8 g, 80%). Elemental analysis: Found: C, 48.00; H, 8.90; N, 4.50%. Calculated for
125 C₁₂H_{24.4}BrNO_{2.2} (MW = 299.85 g·mol⁻¹): C, 48.07; H, 8.87; N, 4.67%. ¹H NMR, δ/ppm (300 MHz,
126 DMSO-*d*₆): 1.19 [12 H, m, CH₃(β+b)]; 1.88 [2 H, m, CH₂(2)]; 2.45 [2 H, t, H₂(3)]; 3.15 [2 H, t,
127 CH₂(1)]; 3.24 [6H, q, CH₂(a)]; 4.08 [2 H, q, CH₂(α)]. ¹³C NMR, δ/ppm (75.47 MHz, DMSO-*d*₆): δ 14.1
128 [CH₃(b)]; 19.6 [CH₃(β)]; 23.5 [CH₂(2)]; 58.0 [CH₂(a)], 60.7 [CH₂(1)]; 62.7 [CH₂(α)]; 172.4 [C=O(4)].
129 ESI-MS, m/z Found (Calculated): 216.1_ (216.34) [C₁₂H₂₆NO₂⁺]; 115.08 (115.15) [C₆H₁₁O₂⁺] IR (v/cm⁻¹)
130 ¹): 3400 (ν_{O-H}); 2950, 2865 (ν_{C-H}); 1725 (ν_{C=O}); 1280 (ν_{C-N}).

131 2.2.2.2. N,N,N-tri(*n*-propyl)(4-ethoxy-4-oxobutyl)-1-aminium bromide ([Pr₃NC₄]Br · 0.7 H₂O)

132 Yield (62.5 g, 81%). Elemental analysis: Found: C, 51.50; H, 9.60; N, 4.20%. Calculated for
133 C₁₅H_{33.4}BrNO_{2.7} (MW = 350.94 g·mol⁻¹): C, 51.34; H, 9.59; N, 3.99%. ¹H NMR, δ/ppm (300 MHz,
134 DMSO-*d*₆): 0.90 [9 H, t, CH₃(c)]; 1.20 [3 H, t, CH₃(β)]; 1.65 [6 H, m, CH₂(b)]; 1.81 [2 H, m, CH₂(2)];
135 2.43 [2 H, t, CH₂(3)]; 3.20 (8 H, m, CH₂(a+1)]; 4.08 (2 H, q, CH₂(α)]. ¹³C NMR, δ/ppm (75.47 MHz,

136 DMSO-*d*₆): 11.1 [CH₃(c)]; 14.4 [CH₃(β)]; 15.2 [CH₂(b)]; 16.8 [CH₂(2)]; 30.1 [CH₂(3)]; 59.7
137 [CH₂(a+1)]; 60.7 [CH₂(α)]; 172.4 [C=O(4)]. ESI-MS, *m/z* Found (Calculated): 258.24 (258.42)
138 [C₁₅H₃₂NO₂⁺]; 115,08 (115,15) [C₆H₁₁O₂⁺] IR (v/cm⁻¹): 3450 (ν_{O-H}); 2957, 2866 (ν_{C-H}); 1728 (ν_{C=O});
139 1285 (ν_{C-N}).

140

141 **2.2.3. N,N,N-tri(*n*-butyl)(4-ethoxy-4-oxobutyl)-1-aminium bromide ([Bu₃NC₄]Br)**

142 To tri(*n*-butyl)amine (68.9 g, 0.35 mol) in 110 mL of ethyl acetate, it was added (42.9 g, 0.22 mol) 4-
143 bromobutyrate acid in 100 mL of ethyl ester, under stirring. The mixture was refluxed for 48h and then
144 stirred at room temperature for 2h. The solution separates into two phases, and the bottom phase
145 corresponding to the brownish oil was recovered, and washed three times with 100 mL of ethyl acetate,
146 and then kept in the freezer for 48 h. The white product, which crystallized after 48 hours, was
147 successively washed with ethyl acetate and diethyl ether, and then dried under vacuum. Yield (71.1 g,
148 85%). Elemental analysis: Found: C, 57.04; H, 9.90; N, 3.50%. Calculated for C₁₈H₃₈BrNO₂ (MW =
149 380.41 g·mol⁻¹): C, 56.83; H, 10.07; N, 3.68%. ¹H NMR (300 MHz, DMSO-*d*₆): 0.94 [9 H, t, CH₃(d)];
150 1.21 [3 H, t, CH₃(β)]; 1.37 [6 H, m, CH₂(c)]; 1.64 [6 H, m, CH₂(b)]; 1.89 [2 H, m, CH₂(2)]; 2.43 [2 H, t,
151 CH₂(3)]; 3.21 [8 H, m, CH₂(a+1)]; 4.09 [2 H, q, CH₂(α)]. ¹³C NMR, δ/ppm (75.47 MHz, DMSO-*d*₆):
152 14.1 [CH₃(d)]; 19.6 [CH₃(β)], 23.5 [CH₃(c)]; 33.1 [CH₂(2)]; 56.8 [CH₂(b)]; 58.0 [CH₂(3)]; 60.7
153 [CH₂(1+a)]; 62.7 [CH₂(α)]; 172.2 [C=O(4)]. ESI-MS, *m/z* Found (Calculated): 300.27 (300.50)
154 [C₁₈H₃₈NO₂⁺]; 115.08 (115.15) [C₆H₁₁O₂⁺] IR (v/cm⁻¹): 2960, 2872 (ν_{C-H}); 1728 (ν_{C=O}); 1283 (ν_{C-N}).

155

156 **2.2.4. Tri(*n*-butyl)(4-ethoxy-4-oxobutyl)-1-phosphonium bromide ([Bu₃PC₄]Br)**

157 Tri(*n*-butyl)[4-ethoxy-4-oxobutyl]phosphonium bromide was synthesized as described for N,N,N-tri(*n*-
158 butyl)(4-ethoxy-4-oxobutyl)-1-aminium bromide using tri(*n*-butyl)phosphine (65.2 g, 0.35 mol) as
159 amine. Yield (73.4 g, 84%). Elemental analysis: Found: C, 54.36; H, 9.85%. Calculated for
160 C₁₈H₃₈BrPO₂ (MW = 397.37 g·mol⁻¹): C, 54.42; H, 9.58%. ¹H NMR (300 MHz, DMSO-*d*₆): 0.90 [9H, t,
161 CH₃(d)]; 1.24 [3H, t, CH₃(β)]; 1.40 [12H, m, CH₂(b+c)]; 1.76 [2H, m, CH₂(2)]; 2.25 [8H, m, CH₂(a+1)];
162 2.50 [2H, m, CH₂(3)]; 4.10 [2H, q, CH₂(α)]. ¹³C NMR, δ/ppm (75,47 MHz, DMSO-*d*₆): 13.3 [CH₃(d)];
163 14.1 [CH₃(β)]; 23.4 [CH₂(c)]; 23.7 [CH₂(b)];, 33.6, [CH₂(2)]; 58.0 [CH₂(3)]; 60.6 [CH₂(1+a)]; 62.7
164 [CH₂(α)]; 169.1 (C=O(4)). ESI-MS, *m/z* Found (Calculated): 317.25 (317.47) [C₁₈H₃₈PO₂⁺]; 259.24
165 (259.97) [C₁₁H₂₉PO₂⁺]. IR (v/cm⁻¹): 2960, 2928, 2874 (ν_{C-H}); 1727 (ν_{C=O}); 1233 (ν_{C-N}).

166

167 The full name, abbreviation and chemical structure of the synthesized AGB-ILs are summarized in
168 Table 2.

169

170 **Table 2.**

171 Name, abbreviation, chemical structure and molecular weight of the synthesized AGB-ILs, and of two
 172 commercial ILs investigated for comparison purposes.

173

Name	Abbreviation	Chemical Structure and Atoms Identification	Molecular Weight (g.mol ⁻¹)
1-(4-ethoxy-4-oxobutyl)-1-methylpyrrolidin-1-ium bromide	[MepyrNC ₄]Br		280.22
N,N,N-triethyl(4-ethoxy-4-oxobutyl)-1-aminium bromide	[Et ₃ NC ₄]Br		296.25
N,N,N-tri(<i>n</i> -propyl)(4-ethoxy-4-oxobutyl)-1-aminium bromide	[Pr ₃ NC ₄]Br		338.33
N,N,N-tri(<i>n</i> -butyl)(4-ethoxy-4-oxobutyl)-1-aminium bromide	[Bu ₃ NC ₄]Br		380.41
Tri(<i>n</i> -butyl)(4-ethoxy-4-oxobutyl)-1-phosphonium bromide	[Bu ₃ PC ₄]Br		397.37
Tetra(<i>n</i> -butyl)ammonium bromide	[N ₄₄₄₄]Br		324.41
Tetra(<i>n</i> -butyl)phosphonium bromide	[P ₄₄₄₄]Br		341.37

174

175

176 **2.3. Characterization of AGB-ILs**

177 All IL samples were dried under vacuum (10 Pa) at room temperature for a minimum of 48h before
178 carrying out their characterization. The water content of the dried ILs was determined by Karl Fischer
179 coulometry using a Metrohm 787 KF Titrino coulometer with Hydranal 34805 and Hydranal 37817
180 (from Fluka) as titrant; their water concentration was less than 6×10^{-4} in weight fraction. During the
181 preparation of the ILs aqueous solutions for the ecotoxicity assays and ternary phase diagrams
182 determination, the water content of each IL was taken into account. Elemental analyses (C, H, N and S
183 contents) of all synthesized ILs were carried on a Perkin-Elmer 2400 C, H, N and S element analyzer.
184 Infra-Red (IR) spectra were recorded at room temperature with a PerkinElmer UATR Two
185 spectrometer. ^1H and ^{13}C Nuclear magnetic resonance (NMR) were recorded at room temperature with
186 a Bruker AC 30 spectrometer (250 MHz for ^1H , 62.5 MHz for ^{13}C) using $\text{DMSO-}d_6$ as solvent.
187 Chemical shifts (in ppm) for ^1H and ^{13}C NMR spectra are referenced to residual protic solvent peaks.
188 Electrospray ionization mass spectrometry (ESI-MS) of AGB-ILs diluted in methanol were obtained on
189 a hybrid tandem quadrupole/time-of-flight (Q-TOF) instrument, equipped with a pneumatically assisted
190 electrospray (Z-spray) ion source (Micromass, Manchester, UK) operated in positive mode; the
191 capillary voltage was 3500 V; and the extraction cone voltage varied between 30-60V with the flow of
192 injection of 5 mL/min. The decomposition temperatures of the ILs were determined by
193 thermogravimetric analyses (TGA) using a Netzsch TG 209 F3 Tarsus thermogravimetric analyzer,
194 under nitrogen atmosphere, with samples of 10-20 mg. These were heated from 30 °C to 500 °C, with a
195 heating rate of 10 °C·min⁻¹. Differential Scanning Calorimetry (DSC) experiments were performed with
196 a TA Instruments Q100, under nitrogen atmosphere, with a cooling and heating rate of 10 °C·min⁻¹.

197

198 **2.4. Microtox[®] acute toxicity tests**

199 To address the ecotoxicity of the synthesized AGB-ILs, the standard Microtox[®] liquid-phase assay [36]
200 was used, in which it is evaluated the luminescence inhibition of the bacteria *Allvibrio fischeri* (strain
201 NRRL B-11177) [37]. In this work, the standard 81.9% test protocol was followed [38]. The
202 microorganism was exposed to a range of diluted aqueous solutions of each IL (from 0 to 81.9 wt%),
203 where 100% of AGB-IL corresponds to a known concentration of a stock solution previously prepared
204 [39]. After 5, 15 and 30 min of exposure of the bacterium to each IL aqueous solutions, the light output
205 of the bacterium was assessed and compared with the light output of the blank control (an aqueous
206 solution without AGB-ILs), enabling the calculation of the EC₅₀ values at 5, 15 and 30 min through the
207 Microtox[®] Omni™ Software [39].

208

209 **2.5. ABS phase diagrams**

210 Aqueous solutions of each IL ([MepyrNC₄]Br, [Et₃NC₄]Br, [Pr₃NC₄]Br, [Bu₃NC₄]Br, [Bu₃PC₄]Br) at

242 Information. All the synthesized ILs have melting points below 100 °C, i.e. from 73 to 90 °C, which is
 243 attributed to the bulky and asymmetric cation with high charge dispersion, and thus to the poor cation-
 244 anion interactions. Furthermore, the melting points slightly increase with the alkyl chain at the cation, in
 245 agreement with the literature [44]. On the other hand, [Bu₃PC₄]Br (T_m = 88 °C) shows a lower melting
 246 point than the corresponding ammonium salt [Bu₃NC₄][Br] (T_m = 90 °C). The same behaviour, observed
 247 with other ammonium- and phosphonium-based ILs including the commercial ones ([N₄₄₄₄][Br] with T_m
 248 = 104 °C and [P₄₄₄₄][Br] with T_m = 101 °C), was attributed to the larger radius of the phosphorus atom
 249 leading to a higher dispersion of charge [45]. It is known that the glass transition temperature is
 250 approximately two-thirds of the melting point value [46]. The range of experimental T_g/T_m ratio was
 251 found to be between 0.58 and 0.78 for different molecules and polymers [47]. The T_g/T_m of the prepared
 252 ILs (given in Table 3) ranges between 0.64 and 0.72, fitting within the range of values reported in the
 253 literature [47].

254

255 **Table 3**

256 Melting (T_m), glass transition (T_g) and decomposition (T_{dec}) temperatures for the synthesized AGB-ILs.

257

AGB-ILs	T _m (°C) ^a	T _g (°C)	T _g /T _m	T _{dec} (°C)
[MepyrNC ₄]Br	73	-31	0.70	179
[Et ₃ NC ₄]Br	78	-21	0.72	187
[Pr ₃ NC ₄]Br	79	-	-	184
[Bu ₃ NC ₄]Br	90	-40	0.64	198
[Bu ₃ PC ₄]Br	88	-	-	310

263

264

265

(a) The uncertainty in the measured temperature was (± 0.2 °C).

266

267

268

269

270

271

272

273

274

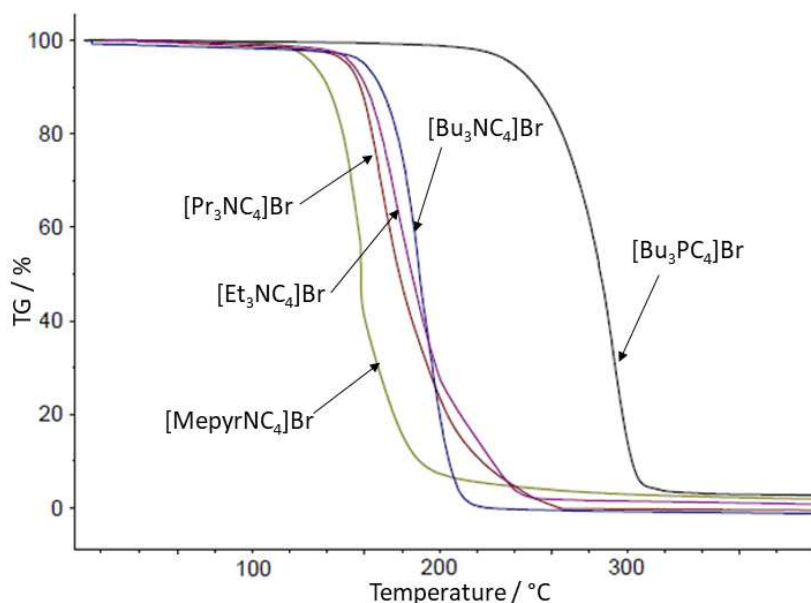
275

276

277

The thermal stability of the synthesized AGB-ILs was determined by TGA over the temperature range between 30 and 400 °C, being the respective data given in Table 3. The thermal degradation profile of the investigated ILs is shown in Figure 2, where the decomposition temperature (T_{dec}) of all these salts falls in the range between 180 and 310 °C (Figure 2). The ILs thermal stabilities increase in the order: [MepyrNC₄]Br < [Pr₃NC₄]Br < [Et₃NC₄]Br < [Bu₃NC₄]Br << [Bu₃PC₄]Br. With the exception of [Pr₃NC₄]Br IL (T_{dec} = 184 °C), a slight increase in the thermal stability is observed when increasing the cation alkyl chain length. In addition, the cyclic ammonium [MepyrNC₄]Br is the IL with the lowest T_{dec} confirming that the thermal stability of these ILs mostly depends on the number of carbon atoms at the cation. For the ILs comprising ammonium cations, the maximum degradation temperature is obtained with the *n*-butyl groups. Furthermore, the tri(*n*-butyl)phosphonium-based IL is more thermally stable than the respective ammonium counterpart ([Bu₃NC₄]Br with T_{dec} = 198 °C *versus* [Bu₃PC₄]Br with T_{dec} = 310 °C). These results are in agreement with those of other

278 ammonium/phosphonium-based ILs, where phosphonium-based ILs present higher values of T_{dec} [48,
279 49]. Tsunashima *et al.* [50] attributed this increase to the presence of empty d-orbitals on the
280 phosphorus atom.
281



282
283 **Fig. 2.** TGA profiles for bromide based AGB-ILs.
284

285 The five AGB-ILs were tested in terms of their effect against the marine luminescent bacteria *Allvibrio*
286 *fischeri*. The EC_{50} values determined after 5, 15 and 30 min of exposure, and the respective 95%
287 confidence limits, are reported in Table 4. The EC_{50} data at 30 min were adopted to ensure enough
288 exposition time to verify the full effect in the luminescence inhibition [51]. The EC_{50} values at the same
289 times of exposure for the commercial tetrabutylammonium and tetrabutylphosphonium bromide ILs
290 ($[N_{4444}]Br$, $[P_{4444}]Br$) [52] are also displayed in Table 4 for comparison purposes. The higher the EC_{50}
291 values the less toxic is the IL towards this luminescent marine bacteria. Regardless of the exposure
292 time, the results obtained show that the toxicity of AGB-ILs toward the bacteria increase according to
293 the following sequence: $[MepyrNC_4]Br < [Et_3NC_4]Br < [Pr_3NC_4]Br < [Bu_3NC_4]Br \ll [Bu_3PC_4]Br$.
294 Because all AGB-ILs share the bromide anion, the differences in their toxicity are a result of the IL
295 cation. For the ammonium-based ILs, the toxicity increases with the alkyl chain length increase, being
296 this a well-known trend recurrently named as the “side-chain effect” [53, 54]. The increase of the cation
297 alkyl chain length leads to an increase of its hydrophobicity/lipophilicity, resulting in a higher ability to
298 interact with and/or permeate phospholipid bilayers. Taking into account the cation central atom, the
299 EC_{50} values decrease from $[Bu_3NC_4]Br$ to $[Bu_3PC_4]Br$, meaning that the ammonium-based IL is less
300 toxic than its phosphonium-based counterpart, being in agreement with previous findings [55]. The
301 same behavior is shown for the commercial ILs ($[N_{4444}]Br$ vs. $[P_{4444}]Br$). In general, all AGB-ILs
302 synthesized and proposed in this work display a lower toxicity to *Allvibrio fischeri* than those

303 commonly used, namely [N₄₄₄₄]Br and [P₄₄₄₄]Br. All the studied AGB-ILs can be considered as
 304 harmless or practically harmless (at 30 min of exposure: 191 mg.L⁻¹ ≤ EC₅₀ ≤ 3052 mg.L⁻¹) according to
 305 Passino and Smith classification [56].

306 **Table 4**

307 Microtox[®] EC₅₀ values (mg.L⁻¹) for *Allvibrio fischeri* after 5, 15 and 30 min of exposure to aqueous
 308 solutions of AGB-ILs and of two commercial ILs [51, 52] with the respective 95% confidence limits (in
 309 brackets).

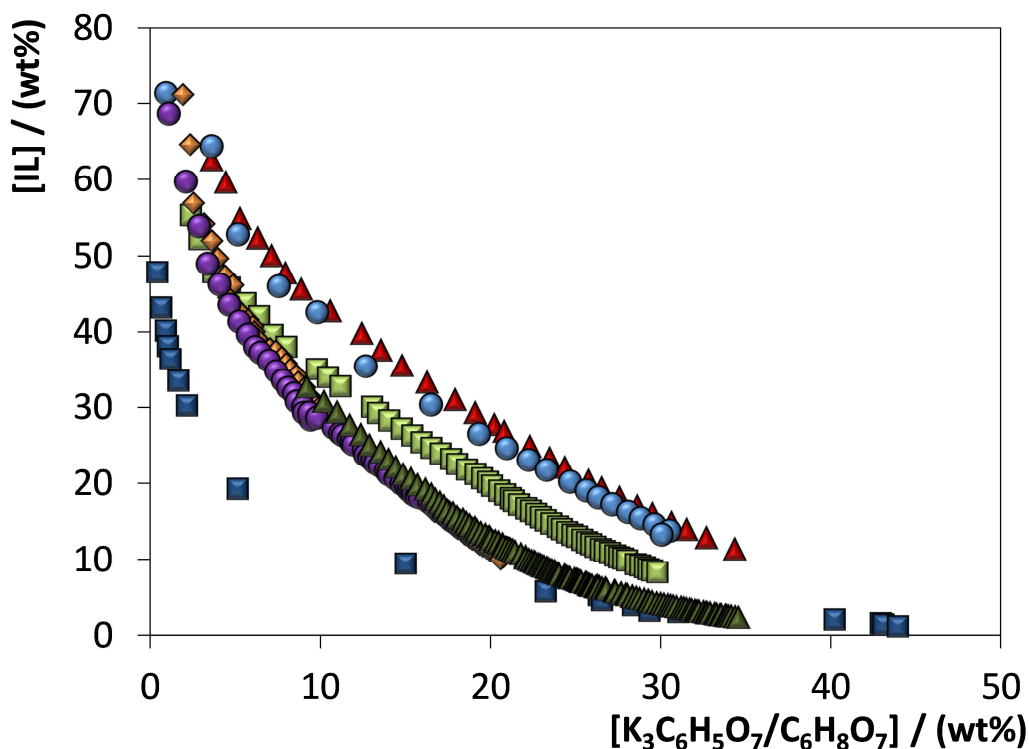
AGB-ILs	EC ₅₀ (mg.L ⁻¹) (lower limit; upper limit)		
	5 min	15 min	30 min
[MePyrNC ₄]Br	3058.56 (1596.73; 4478.39)	3052.29 (2277.68; 4526.90)	3052.32 (1882.86; 4281.78)
[Et ₃ NC ₄]Br	2664.15 (1917.81; 3410.5)	2491.05 (1627.56; 3354.54)	2415.00 (1621.30; 3208.70)
[Pr ₃ NC ₄]Br	2157.05 (1678.50; 2635.61)	2026.41 (1411.48; 2641.35)	2018.72 (1267.08; 3630.37)
[Bu ₃ NC ₄]Br	435.43 (295.60; 575.27)	380.92 (260.06; 501.78)	327.22 (317.22; 336.78)
[Bu ₃ PC ₄]Br	351.76 (248.71; 454.83)	243.95 (239.41; 370.06)	191.30 (141.25; 200.45)
[N ₄₄₄₄]Br	233.30 (223.36; 243.15)	160.22 (143.55; 176.87)	-
[P ₄₄₄₄]Br	216.00 (21.60; 1382.40)	172.80 (0.00; 3218.40)	-

311
312

313 3.2. ABS phase diagrams

314 The novel AGB-ILs proposed in this work have low melting points, below 100 °C, display high
 315 degradation temperatures (180-310 °C), and low toxicity as shown by being harmless or practically
 316 harmless towards the marine bacteria *Allvibrio fischeri*. Therefore, their use in a wide range of
 317 applications can be envisioned. Aiming at exploring their use in liquid-liquid separation processes, we
 318 addressed here their potential to form ABS with salts. Novel ternary phase diagrams were determined
 319 for all the AGB-ILs + water + potassium citrate/citric acid mixtures (K₃C₆H₅O₇/C₆H₈O₇ mixtures, pH =
 320 7.0) at 25°C and atmospheric pressure. In the respective phase diagrams, illustrated in Figure 3, the
 321 biphasic region is localized above the solubility curve described by the experimental solubility data
 322 points. Diagrams with a larger area above the binodal curve have therefore a higher ability to form two
 323 phases, i.e. the IL is more easily salted-out by the citrate-based salt [57]. For comparison purposes, the
 324 ternary phase diagrams for the commercial [N₄₄₄₄]Br and [P₄₄₄₄]Br under the same conditions, which
 325 were previously reported [51, 52], are also provided. The corresponding experimental weight fraction
 326 data are given in the **Tables S1-S5 in the** Supporting Information. All the calculations considering the

327 weight fraction of the phase-forming components were performed discounting the complexed water in
328 the commercial citrate-based salt and citric acid.



329
330

331 **Fig. 3.** Ternary phase diagrams, in an orthogonal representation, for the systems composed of IL +
332 water + $K_3C_6H_5O_7/C_6H_8O_7$ buffered at pH = 7.0 and at 25°C: [MepyrNC₄]Br (▲); [EtNC₄]Br (●);
333 [PrNC₄]Br (■); [BuNC₄]Br (◆); [Bu₃PC₄]Br (●), [N₄₄₄₄]Br (▲) [57]; [P₄₄₄₄]Br (■) [58].

334 The phase diagrams shown in Figure 3 allow the evaluation of the effect of the ammonium alkyl
335 chain length, the effect of the IL central atom (N vs. P), and the presence of cyclic cation structures
336 against linear alkyl side chains. All studied compounds comprise the bromide anion, being the
337 difference in liquid-liquid demixing a result of the IL cation nature. The capacity of AGB-ILs to form
338 ABS (or to be salted-out by the organic citrate-based salt) follows the order: [Bu₃PC₄]Br > [Bu₃NC₄]Br
339 > [Pr₃NC₄]Br > [Et₃NC₄]Br ≈ [MepyrNC₄]Br. It is shown that the increase of the cation alkyl chain
340 length facilitates the creation of ABS, meaning that longer alkyl side chain ILs are more easily salted-
341 out by the organic salt, in agreement with literature data and demonstrating that this behavior is
342 independent of the salt used [59-61]. On the other hand, [MepyrNC₄]Br is the IL with the lowest ability
343 to create ABS, as result of its higher hydrophilicity afforded by a lower number of methylene groups.
344 The phase diagrams for the systems composed of [Bu₃NC₄]Br and [Bu₃PC₄]Br are also presented in
345 Figure 3, allowing to appraise the effect of the IL cation central atom. Although with a similar chemical
346 structure, [Bu₃PC₄]Br presents a slightly better separation performance in presence of aqueous solutions
347 of $K_3C_6H_5O_7/C_6H_8O_7$, in agreement with what has been previously demonstrated with other salts [62-
348 64] and in agreement with the trend observed with the commercial ILs [P₄₄₄₄]Br and [N₄₄₄₄]Br. Both the

349 IL pairs $[\text{Bu}_3\text{PC}_4]\text{Br}/[\text{Bu}_3\text{NC}_4]\text{Br}$ and $[\text{P}_{4444}]\text{Br}/[\text{N}_{4444}]\text{Br}$ comprise the bromide anion, and the
350 differences in the respective phase diagrams are a result of the charge distribution at the IL cation
351 central heteroatom which dictates the IL affinity for water [45]. In summary, amongst the AGB-ILs
352 investigated, $[\text{MepyrNC}_4]\text{Br}$ displays the lowest capacity to create ABS and requires a higher amount of
353 citrate-based salt to undergo phase separation, whereas $[\text{Bu}_3\text{PC}_4]\text{Br}$ is the most effective AGB-IL and
354 requires the lowest amount of $\text{K}_3\text{C}_6\text{H}_5\text{O}_7/\text{C}_6\text{H}_8\text{O}_7$ to form ABS. The fitting of the experimental binodal
355 curves, and the determination of tie-line data and respective length were additionally performed, being
356 provided in the Supporting Information (Tables S6 and S7). Even though there are 4 ions in solution,
357 ion exchange is not expected to occur since the probability of different ion pairs to form is significantly
358 low, as previously confirmed with ABS formed by ionic liquids and strong salting-out salts [65-66],
359 being this the case of the current work.

360 In summary, it is here shown that AGB-ILs form ABS with $\text{K}_3\text{C}_6\text{H}_5\text{O}_7/\text{C}_6\text{H}_8\text{O}_7$ at controlled pH
361 (7.0). In addition, their high thermal stability and low ecotoxicity against *Allvibrio fischeri* support their
362 further investigation in other ABS to be applied in separation processes of labile biomolecules.

363

364 4. Conclusions

365 In this work, we reported the synthesis and characterization of five new water-soluble analogues of
366 glycine-betaine-based ionic liquids (AGB-ILs) combined with the bromide anion. Their thermal
367 properties, namely melting temperature, glass transition temperature and decomposition temperature
368 were determined and discussed in terms of the IL chemical structure. All synthesized AGB-ILs fit
369 within the ILs category, with a melting temperature below 100 °C, and present high degradation
370 temperatures (180-310 °C). Their toxicity against the marine luminescent bacteria *Allvibrio fischeri*
371 showed that the studied AGB-ILs are harmless or practically harmless and display a lower toxicity of
372 this marine bacteria than commonly used ILs, such as $[\text{N}_{4444}]\text{Br}$ and $[\text{P}_{4444}]\text{Br}$. Given the AGB-ILs
373 properties, we studied their potential to create ABS that could be applied in separation processes. The
374 ABS phase diagrams were determined for systems composed of AGB-IL + water + $\text{K}_3\text{C}_6\text{H}_5\text{O}_7/\text{C}_6\text{H}_8\text{O}_7$
375 at pH 7.0 and at 25 °C. The obtained results confirm their high ability to be salted-out by the organic
376 salt and to form ABS, where more hydrophobic ILs more easily form two-phase systems or require a
377 lower amount of salt to undergo phase separation in aqueous media. This ability to be salted-out by the
378 organic salt follows the order $[\text{Bu}_3\text{PC}_4]\text{Br} > [\text{Bu}_3\text{NC}_4]\text{Br} > [\text{Pr}_3\text{NC}_4]\text{Br} > [\text{Et}_3\text{NC}_4]\text{Br} \approx [\text{MepyrNC}_4]\text{Br}$.
379 All the properties shown for the newly reported AGB-ILs are beneficial to develop sustainable and
380 biocompatible separation processes.

381

382 Acknowledgments

383 This work was developed within the scope of the project CICECO-Aveiro Institute of Materials, FCT
384 Ref. UID/CTM/50011/2019, financed by national funds through the FCT/MCTES. M. M. Pereira
385 acknowledges the PhD grant (2740-13-3) and financial support from Coordenação de Aperfeiçoamento
386 de Pessoal de Nível Superior – Capes and the Short Term Scientific Mission grant COST-STSM-
387 ECOST-STSM-CM1206–011015-066583. M. G. Freire acknowledges the European Research Council
388 under the European Union’s Seventh Framework Programme (FP7/2007-2013)/ERC Grant 337753. We
389 acknowledge D. Harakat for the ESI-MS measurements.

390

391 **References**

- 392 [1] A. Schmid, A. Koller, R.G. Mathys, B. Withot, *Extremophiles* 2 (1998) 249-256.
- 393 [2] T.P.T. Pham, C.W. Cho, Y.S. Yun, *Water Research* 44 (2010) 352-372.
- 394 [3] P. Wasserscheid and W. Keim, *Angew. Chem., Int. Ed.* 39 (2000) 3772-3789.
- 395 [4] M.J. Earle, K.R. Seddon, *Pure Appl. Chem.* 72 (2000) 1391-1398.
- 396 [5] J.L. Anderson, J. Ding, T. Welton, D.W. Armstrong, *J. Am. Chem. Soc.* 124 (2002) 14247-
397 14254.
- 398 [6] J. Dupont, R.F. De Souza, P.A.Z. Suarez, *Chem. Rev.* 102 (2002) 3667-3692).
- 399 [7] A. Jordan, N. Gathergood, *Chem. Soc. Rev.*, 44 (2015) ,8200-8237.
- 400 [8] D.O. Hartmann, C.S. Pereira, *Toxicity of Ionic Liquids: Past, Present, and Future, Ionic Liquids*
401 *in Lipid Processing and Analysis - Opportunities and Challenges*, 2016, Chapter 13, Pages 403-
402 421.]
- 403 [9] M. Amde, J.-F. Liu, L. Pang, *Environ. Sci. Technol.* 49 (2015) 12611–12627.
- 404 [10] S.T. Handy, *Chem. Eur. J.* 9 (2003) 2938-2944.
- 405 [11] D.-J. Tao, Z. Cheng, F.-F. Chen, Z.-M. Li, N. Hu, X.-S. Chen, *J. Chem. Eng. Data* 58 (2013),
406 1542–1548.
- 407 [12] N. Muhammad, M.I. Hossain, Z. Man, M. El-Harbawi, M. A. Bustam, Y. Ab. Noaman, N.B.M.
408 Alitheen, M.K. Ng, G. Hefter, C.-Y. Yin, *J. Chem. Eng. Data* 57 (2012) 2191–2196.
- 409 [13] R. Vijayaraghavan, B.C. Thompson, D.R. MacFarlane, R. Kumar, M. Surianarayanan, S.
410 Aishwarya, P.K. Sehga, *Chem. Commun.* 46 (2010) 294–296.
- 411 [14] Y-X. An, M.-H. Zong, H. Wu, N. Li, *Bioresour. Technol.* 192 (2015) 165–171.
- 412 [15] S. Yuan, Y. Chen, X. Ji, Z. Yang, X. Lu, *Fluid Phase Equilib.* 445 (2017) 14-24.
- 413 [16] P. Moriel, E. J. García-Suárez, M. Martínez, A. B. García, M. A. Montes-Morán, V. Calvino-
414 Casilda, M. A. Bañares, *Tetrahedron Lett.* 51 (2010) 4877–4881.
- 415 [17] S. Hu, T. Jiang, Z. Zhang, A. Zhu, B. Han, J. Song, Y. Xie, W. Li , *Tetrahedron Lett.* 48 (2007)
416 5613–5617.

- 417 [18] D.-J.Tao, Z. Cheng, F.-F. Chen, Z.-M. Li, N. Hu, X.-S. Chen, *J. Chem. Eng. Data* 58 (2013) 58
418 1542–1548.
- 419 [19] X.-D. Hou, T.J. Smith, N. Li, M.-H. Zong, *Biotechnol. Bioeng.* 109 (2012) 2484-2493.
- 420 [20] Poletti, C. Chiappe, L. Lay, D. Pieraccini, L. Polito, G. Russo, *Green Chem.* 9 (2007) 337–341.
- 421 [21] A. K. Jha, N. Jain, *Tetrahedron Lett.* 54 (2013) 4738–4741.
- 422 [22] Y. De Gaetano, A. Mohamadou, S. Boudesocque, J. Hubert, R. Plantier-Royon, L. Dupont, J.
423 *Mol Liq.* 207 (2015) 60-66.
- 424 [23] A. Messadi, A. Mohamadou, S. Boudesocque, L. Dupont, P. Fricoteaux, A. Nguyen-Van-Nhien,
425 M. Courty, *J. Mol Liq.* 184 (2013) 68-72.
- 426 [24] Y. De Gaetano, J. Hubert, A. Mohamadou, S. Boudesocque, R. Plantier-Royon, J.H. Renault, L.
427 Dupont, *Chem. Eng. J.* 285 (2016) 596-604.
- 428 [25] A. Messadi, A. Mohamadou, S. Boudesocque, L. Dupont, E. Guillon, *Sep. Purif. Technol.* 107
429 (2013) 172-178. 31.
- 430 [26] Y. Zhou, S.Boudesocque, A.Mohamadou, L. Dupont, *Sep. Sci. Technol.* 50 (2015) 38-44.
- 431 [27] S. Boudesocque, A. Mohamadou, L. Dupont, *New J. Chem.*, 38 (2014) 5573-5581.
- 432 [28] A. M. Ferreira, E. S. Morais, A. C. Leite, A. Mohamadou, B. Holmbom, T. Holmbom, B. M.
433 Neves, J. A. P. Coutinho, M. G. Freire, A. J. D. Silvestre, *Green Chem.* 19 (2017) 2626-2635.
- 434 [29] D. Coleman and N. Gathergood, *Chem. Soc. Rev.* 39 (2010) 600–637
- 435 [30] A. Sakamoto, N. Murata, *Plant, Cell Environ.* 25 (2002) 163-171.
- 436 [31] M. Ashraf, M.R. Foolad, *Environ. Exp. Bot.* 59 (2007) 206-216.
- 437 [32] J. R. Hoffman, N. A. Ratamess, J. Kang, S. L. Rashti and A. D. Faigenbaum, *J. Int. Soc. Sports*
438 *Nutr.* 6 (2009) 7-7.
- 439 [33] Z. F. Nsimba, M. Paquot, L. G. Mvumbi and M. Deleu, *Biotechnol. Agron. Soc. Environ.* 14
440 (2010) 737-748.
- 441 [34] S. M. Steinberg, E. J. Poziomek, W. H. Engelmann and K. R. Rogers, *Chemosphere* 30 (1995)
442 155–2197.
- 443 [35] M. Corporation, Microtox[®] manual—a toxicity testing hand-book, Microbics Corporation, 1992,
444 Carlsbad, 1–5.
- 445 [36] S.P.M. Ventura, A.M.M. Gonçalves, F. Gonçalves, J.AP. Coutinho, *Aquat. Toxicol.* 96 (2010)
446 290-297.
- 447 [37] B.T. Johnson, Microtox acute toxicity test in C. blaise J.-F. Férard (Eds), *Small-scale Freshwater*
448 *toxicity Investigation*, Springer, Netherlands, pp. 69-105.
- 449 [38] A. Environmental, Carlsbad CA, USA, 1998.
- 450 [39] Azur Environmental, 1998. Azur Environmental, Microtox Manual. www.azueenv.com.

- 451 [40] C.M.S.S. Neves, S.P.M. Ventura, M.G. Freire, I.M. Marrucho, J.A.P. Coutinho, *J. Phys. Chem.*
452 *B* 113 (2009) 5194–5199.
- 453 [41] S.P.M. Ventura, S.G. Sousa, L.S. Serafim, Á.S. Lima, M.G. Freire, J.A.P. Coutinho, *J. Chem.*
454 *Eng. Data* 56 (2011) 4253–4260.
- 455 [42] H. Passos, A.R. Ferreira, A.F.M. Cláudio, J.A.P. Coutinho, M.G. Freire, *Biochem. Eng. J.*, 67
456 (2012) 68-76.
- 457 [43] J.C. Merchuk, B.A. Andrews, J.A. Asenjo, *J Chromatogr., B: Biomed. Sci. Appl.* 711 (1998)
458 285-293.
- 459 [44] J. D. Holbrey and K. R. Seddon, *J. Chem. Soc., Dalton Trans.* (1999) 2133–2139.
- 460 [45] P.J. Carvalho, S.P.M. Ventura, M.L.S. Batista, B. Schröder, F. Gonçalves, J. Esperança, F.
461 Mutelet, J.A.P. Coutinho *J. Chem. Phys.* 140 (2014) 064505.
- 462 [46] W. Kauzmann, *Chem. Rev.* 43 (1948) 219–256.
- 463 [47] R. G. Beaman, *Polymer Sci.* 9 (1952) 470–472.
- 464 [48] J. Kagimoto, K. Fukumoto, H. Ohno *Chem. Commun.* 2006, 2254–2256
- 465 [49] C. Maton, N. De Vos, C. V. Stevens, *Chem. Soc. Rev.* 42 (2013) 5963-5977.
- 466 [50] K. Tsunashima, S. Kodama, M. Sugiya, Y. Kunugi, *Electrochim. Acta* 56 (2010) 762-766.
- 467 [51] S.P.M. Ventura, C.S. Marques, A.A. Rosatella, C.A.M. Alfonso, F. Gonçalves, J.P.A. Coutinho,
468 *Ecotoxicol. Environ. Saf.* 76 (2012) 162-168.
- 469 [52] M. M. Pereira, J. Gomes, M. R. Almeida, J. A. P. Coutinho, A. Mohamadou, M. G. Freire,
470 *Biotechnol. Prog.* **2018**, 34, 1205-1212.
- 471 [53] S. Stolte, M. Matzke, J. Arning, A. Boschen, W.R. Pitner, U. Welz-Biermann, B. Jastorff, J.
472 Ranke, *Green Chem.* 9 (2007) 1170-1179
- 473 [54] S.P.M. Ventura, A.M.M. Gonçalves, T. Sintra, J. Pereira, F. Gonçalves, J.A.P. Coutinho,
474 *Ecotoxicology* 22 (2013) 1-12.
- 475 [55] D.J. Couling, R.J. Bernot, K.M. Docherty, J.K. Dixon, E.J. Maginn, *Green Chem.* 8 (2006) 82-
476 90.
- 477 [56] D.R.M. Passino, S.B. Smith, *Environ. Toxicol. Chem.* 6 (1987) 901-907.
- 478 [57] F.A. e Silva, T. Sintra, S.P.M. Ventura, J.A.P. Coutinho, *Sep. Purif. Technol.* 122 (2014) 315–
479 322.
- 480 [58] M.M. Pereira, S.N. Pedro, M.V. Quental, Á. S. Lima, J.A.P. Coutinho, M. G. Freire, J.
481 *Biotechnol.* 206 (2015) 17–25.
- 482 [59] C.M.S.S. Neves, S.P.M. Ventura, M.G. Freire, I.M. Marrucho, J.A.P. Coutinho, *J. Phys; Chem.*
483 *B* 113 (2009) 5194-5199.
- 484 [60] A.F.M. Claudio, A.M. Ferreira, S. Shahriari, M.G. Freire, J.A.P. Coutinho, *J. Phys. Chem. B*
485 115 (2011) 11145-11153.

- 486 [61] S.P.M. Ventura, S.G. Sousa, L.S. Serafim, A.S. Lima, M.G. Freire, J.A.P. Coutinho, J. Chem
487 Eng. Data 56 (2011) 4253-4260.
- 488 [62] L.S. Louros, A.F.M. Cláudio, C.M.S.S. Neves, M. G. Freire, I.M. Marrucho, P. Jérôme, J.A.P.
489 Coutinho, Int. J. Mol. Sci. 11 (2010) 1777-1791.
- 490 [63] M.M. Pereira, S.N. Pedro, M.V. Quental, Á.S. Lima, J.A.P. Coutinho, M .G. Freire, J.
491 Biotechnol. 206 (2015) 17-25.
- 492 [64] T.E. Sintra, R. Cruz, S.P.M. Ventura, J.A.P. Coutinho, J. Chem. Thermodyn. 77 (2014) 206-213.
- 493 [65] C.M.S.S. Neves, M.G. Freire, J.A.P. Coutinho, RSC Adv. 2 (2012) 10882-10890.
- 494
- 495 [66] N.J. Bridges, K.E. Gutowski, R.D. Rogers, Green Chem. 9 (2007) 177-183.

Figures captions

Fig. 1. Synthetic route of AGB-ILs.

Fig. 2. TGA profile for bromide based AGB-ILs.

Fig. 3. Ternary phase diagrams, in an orthogonal representation, for the systems composed of IL + water + $\text{K}_3\text{C}_6\text{H}_5\text{O}_7/\text{C}_6\text{H}_8\text{O}_7$ buffered at $\text{pH} = 7.0$ and at 25°C : [MepyrNC₄]Br (▲); [Et□NC₄]Br (●); [Pr□NC₄]Br (■); [Bu□NC□]Br (◆); [Bu₃PC₄]Br (●), [N₄₄₄₄]Br (▲) [57]; [P₄₄₄₄]Br (■) [58].

Tables captions

497

498 **Table 1**

499 Name, CAS-number, molecular weight, purity and suppliers of applied chemicals.

Table 2

500 Name, abbreviation, chemical structure and molecular weight of the synthesized AGB-ILs, and of two
501 commercial ILs investigated for comparison purposes.

Table 3

Melting (T_m), glass transition (T_g) and decomposition (T_{dc}) temperatures for the synthesized AGB-ILs.

Table 4

Microtox[®] EC_{50} values ($mg.L^{-1}$) for *Allvibrio fischeri* after 5, 15 and 30 min of exposure to aqueous solutions of AGB-ILs and of two commercial ILs [51, 52] with the respective 95% confidence limits (in brackets).